Advanced Steel Construction – Vol. 19 No. 4 (2023) 403–410
DOI:10.18057/IJASC.2023.19.4.9

CONFORMATION AND STATIC PERFORMANCE ANALYSIS OF PENTAGONAL THREE-FOUR STRUT HYBRID OPEN-TYPE CABLE DOME

Hui Lv [1, 2, *], De-Wang Liu [1, 4], Shi-Lin Dong [2, 3] and Yan-Fen Zhong [1, 4]

[1] *College of Civil Engineering and Architecture, Nanchang Hangkong University, Nanchang 330063, China*
[2] *Space Structures Research Center, Zhejiang University, Hangzhou 310058, China*
[3] *Zhejiang Provincial Key Laboratory of Space Structures, Zhejiang University, Hangzhou 310058, China*
[4] *Nanchang Hangkong University Smart Construction Research Center, Nanchang 330063, China*
** (Corresponding author: E-mail: lvhui@nchu.edu.cn)*

ABSTRACT

Traditional cable domes exhibit many defects, such as irregular grids and weak circumferential stiffness. This paper proposes a new cable dome and elaborates on the topological form of the new cable dome. Furthermore, the pre-stress state of the structure is deduced by establishing the nodal equilibrium equations. In addition, load states analysis and parametric analysis were conducted using finite element simulations in ANSYS software. The results show that the pre-stress distribution of this structure is reasonable because of the regular grids. Compared to traditional cable domes, the new design shows superior static performance and enhanced circumferential stiffness. As a result, the cables hardly slack under different load conditions. Moreover, it can improve structural stiffness by appropriately adjusting the initial pre-stress, rise-span and thickness-span ratios. Finally, recommended ranges of the above parameters are provided, offering valuable engineering design guidance.

ARTICLE HISTORY

Received: 6 July 2023
Revised: 9 September 2023
Accepted: 12 September 2023

KEYWORDS

Cable dome;
Static performance;
Parametric analysis;
Initial pre-stress;
Rise-span ratio;
Thickness-span ratio

1. Introduction

Large spatial structures have recently been used in public buildings, such as sports venues [1, 2], convention centers [3] and airports. In addition to meeting the functions and appearance requirements, modern large spatial structures pursue higher utilization of material properties and lower economic efficiency. Therefore, the study of cable-stayed structures [4] must be conducted. Cable dome has notable advantages including its lightweight nature and structural aesthetics. It is widely regarded as the main super-span structure form for the future [5]. Cable domes have their origins in the concept of tensegrity structures developed by the renowned architect R. B. Fuller. In the 1980s, D. H. Geiger invented the cable dome structure and implemented it for the first time in practical engineering.

The cable dome consists of tension cables, compressed struts and supports. In contrast to other spatial structures, such as reticulated shells [6] or cable-truss systems [7], initial pre-stress in the cable dome plays an important role in establishing the out-of-plane stiffness of the structure to bear external loads and limit the deformation [8]. However, traditional cable domes often exhibit weak out-of-plane stiffness, making them prone to destabilization under asymmetric loading conditions [9, 10]. To address the problem, M.P. Levy proposed the Levy-type cable dome, which incorporates ridge cables, diagonal cables and struts to form a three-dimensional truss. The stability of the structure was significantly improved. However, the grid of the Levy-type cable dome is irregular, increasing the membrane installation difficulty. To overcome this limitation, Fan et al. improved the Levy-type cable dome and proposed the inclined-strut cable dome [11]. In addition, scholars have proposed alternative methods such as replacing the cable trusses with rigid components [12, 13] or combining reticulated shells with cable domes [14] to enhance stiffness. However, these methods cannot fully utilize the mechanical properties of materials.

The topological form determines the stiffness of the cable dome. Many scholars seek to improve the structural performance of cable domes through topological innovation. Some scholars abandoned the traditional Tensile-Integrity concept and proposed multi-strut cable domes and hybrid cable domes, such as honeycomb-type multi-strut series cable domes[15], drum-shaped honeycomb-type cable domes[16], alternated cable domes with single and double brace struts[17], and other cable domes. Compared to traditional cable domes, these multi-strut and hybrid ones have significant advantages in membrane installation and structural stiffness. Moreover, some scholars have proposed bird-nest-type cable domes [18], sunflower-type cable domes [19], star-type tetrahedral cable domes [20], etc. These innovative cable dome designs enrich the array of available options and give new insights for cable dome selection.

An adaptive cable dome [21] has recently been proposed, equipped with an actuator that enables self-adjustment and the ability to accommodate various loading conditions. While the adaptive cable dome maintains its ability to meet the load requirements by changing its topological form, this method introduces a new approach to enhance structural stiffness.

Research has demonstrated that structural parameters (rise-span ratio, strut cross-sectional area and strut height) are closely associated with the mechanical properties of the structure. Meanwhile, parametric analysis has shown that the structural performance can be improved by limiting these structural parameters within specific ranges [22-24]. Therefore, it is necessary to carry out a parametric analysis.

This paper introduces a novel pentagonal three-four strut hybrid open-type cable dome, which is based on the concept of a multi-strut cable dome. Firstly, the topological form of the new cable dome is elucidated, and the pre-stress state of the structure is determined using nodal equilibrium equations. Secondly, a load state analysis is conducted to study the mechanical response of the structure. Finally, a parametric analysis is performed on the structure. The appropriate ranges for the rise-span ratio, thickness-span ratio and pre-stress level of the cable dome are recommended.

2. Structural configuration and pre-stress state analysis

2.1. Structural configuration

The pentagonal three-four strut hybrid open-type cable dome consists of cables, struts and rigid hoop beams. The topological form is shown in Fig. 1. In contrast to the traditional Tensile-Integrity concept, the new cable dome adopts the multi-strut cable dome concept. The upper chord grid of the structure is pentagonal. Starting from the center of the cable dome and extending towards the outer hoop, the struts are arranged in an alternating pattern of four and three. The struts are connected to form a hoop, and the connections between each substructure are designed to be sufficient. This arrangement helps enhance the circumferential stiffness of the structure and improves its ability to resist asymmetric loads.

A comparison is made between the new and the traditional cable domes in four aspects, as outlined in Table 1. Compared with the Geiger-type cable dome, the struts in the new structural arrangement form a hoop, increasing the circumferential stiffness of the structure. The number of hoop cables in the new structure is twelve fewer than that in the levy-type cable dome. Specifically, the new cable dome comprises 84 struts and 184 cables; resulting in a strut-cable ratio of 1:2.2. Comparatively, the strut-cable ratio is approximately 1:3 in the Geiger-type cable dome and 1:5 in the Levy-type cable dome.

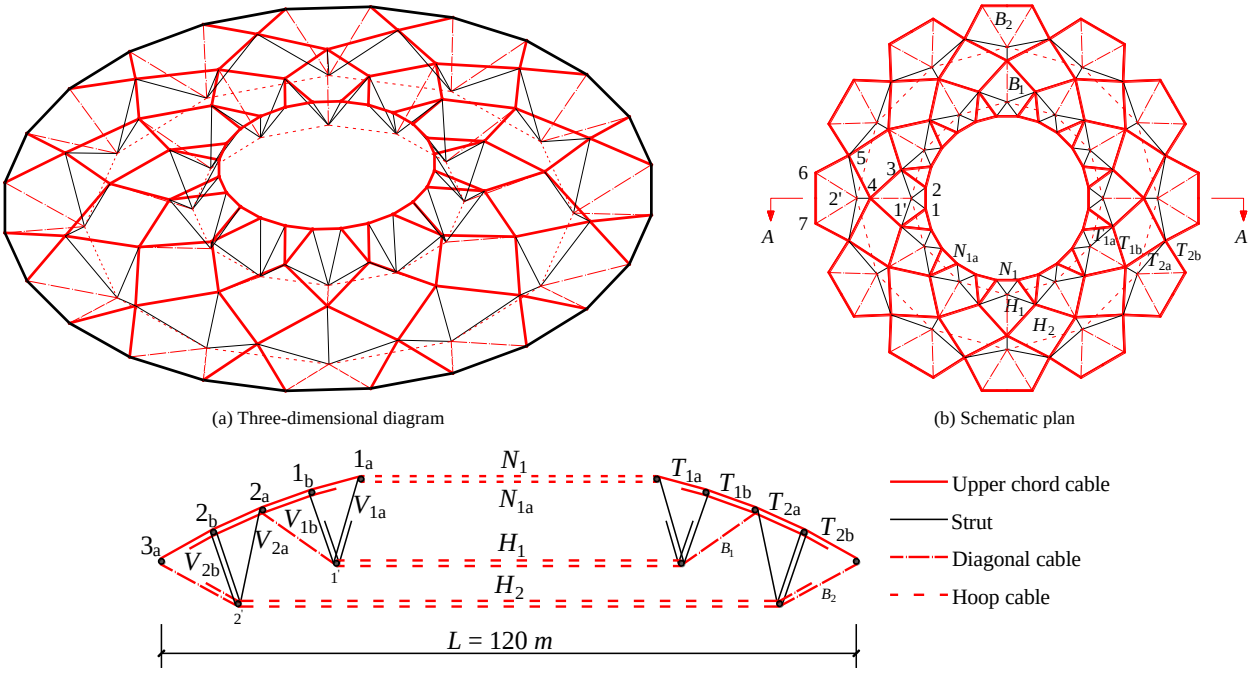

(a) Three-dimensional diagram

(b) Schematic plan

(c) Sectional view (A-A)

Note: H_i-hoop cable; N_1, N_{1a}-upper chord hoop cable; T_{ia}, T_{ib}-ridge cable; B_i-diagonal cable; V_{ia}, V_{ib}-strut; i_a, i_b-upper chord node; i'-lower chord node.

Fig. 1 Schematic diagram of the pentagonal three-four strut hybrid open-type cable dome

Table 1
Comparison of component connected relation

Title	Traditional cable domes		New cable dome
	Geiger-type cable dome	Levy-type cable dome	
Number of components connected to the upper chord node	4	5 or 7	4 or 6
Number of components connected to the lower chord node	4	5	7
Number of diagonal cables per hoop	12	24	12 or 24
Characteristics of the struts	A vertical strut		Struts are arranged by four and three alternately
Characteristics of the horizontal projection of the cables and struts	The projection of the struts is in a discontinuous point system; The projection of diagonal cables coincides with the ridge cable projection		The projection of the ridge cables, diagonal cables and struts are symmetrically distributed along the radial axis

2.2. Pre-stress state analysis

The schematic diagram of the pentagonal three-four strut hybrid open-type cable dome is shown in Fig. 1. In the inner hoop grid, four struts and one diagonal cable intersect at the lower chord node, with one hoop cable passing through the lower chord node. In comparison, three struts and two diagonal cables intersect at the lower chord node in the outer hoop grid. The lower chord node is only positioned along the radial axis of the main grid. The inner hoop upper chord hoop cable is an important feature distinguishing it from other cable domes.

The pentagonal three-four strut hybrid open-type cable dome is symmetrical. Both the plan and section views of the dome are shown in Fig. 2. To facilitate calculations, the tilt angles with the horizontal plane of ridge cable, strut and diagonal cable are denoted as $\alpha_{ia}, \alpha_{ib}, \phi_{ia}, \phi_{ib}, \beta_i$, respectively. The angle between the horizontal projection and radial axis of ridge cable, strut and diagonal cable are denoted as $\gamma_{ia}, \gamma_{ib}, \delta_{ia}, \delta_{ib}, \delta_{i\beta i}$, respectively. Additionally, the upper chord nodes are denoted as i_a, i_b, while the lower chord node is denoted as i' $(i = 1,2)$.

In a substructure with six nodes, l3 equilibrium equations [25] can be formulated. However, since the internal forces of the 14 types of components are unknown, it indicates that the structure is a first-order hyperstatic structure. Suppose the internal force of any one type of member is known. The internal forces of the remaining 13 types of members can be obtained through the nodal equilibrium equations.

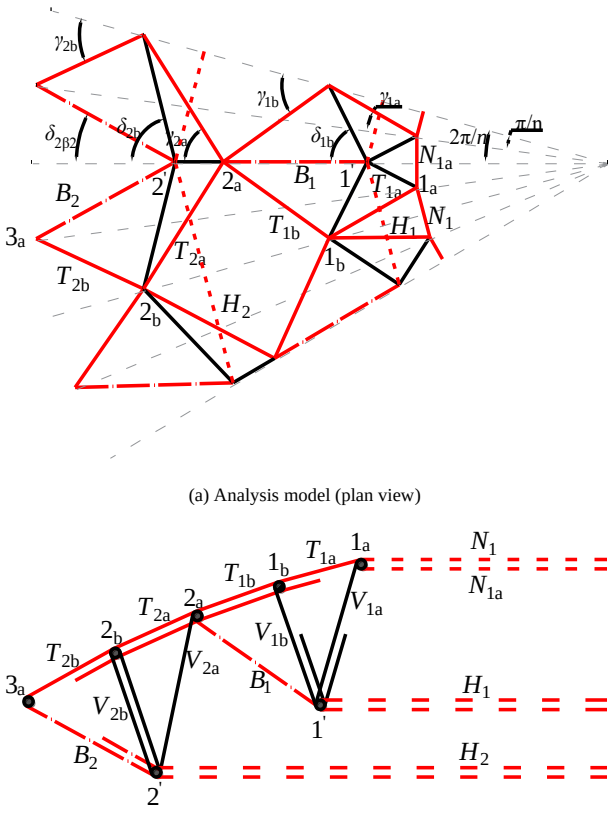

(a) Analysis model (plan view)

(b) Analysis model (section view)

Fig. 2 Analysis model of the pentagonal three-four strut hybrid open-type cable dome

When formulating the nodal equilibrium equations, two equations can be established for nodes located on the radial symmetric axis, while three equations can be established for nodes located off the radial symmetric axis. The nodal equilibrium equation group is as follows:

Node 1_a:

$$\left.\begin{aligned} &T_{1a}\cos\alpha_{1a}\cos\gamma_{1a}+V_{1a}\cos\phi_{1a}\cos\left(\delta_{1a}+\frac{\pi}{n}\right)-N_1\sin\frac{\pi}{n}-N_{1a}\sin\frac{\pi}{n}=0\\ &T_{1a}\cos\alpha_{1a}\sin\gamma_{1a}-V_{1a}\cos\phi_{1a}\sin\left(\delta_{1a}+\frac{\pi}{n}\right)+N_1\cos\frac{\pi}{n}-N_{1a}\cos\frac{\pi}{n}=0\\ &T_{1a}\sin\alpha_{1a}+V_{1a}\sin\phi_{1a}=0\end{aligned}\right\} \quad (1)$$

Node $1'$:

$$\left.\begin{aligned} &-2V_{1a}\cos\phi_{1a}\cos\delta_{1a}+2V_{1b}\cos\phi_{1b}\cos\delta_{1b}+B_1\cos\beta_1-2H_1\sin\frac{2\pi}{n}=0\\ &2V_{1a}\sin\phi_{1a}+2V_{1b}\sin\phi_{1b}+B_1\sin\beta_1=0\end{aligned}\right\} \quad (2)$$

Node 1_b:

$$\left.\begin{aligned} &-2T_{1a}\cos\alpha_{1a}\cos\left(\gamma_{1a}-\frac{\pi}{n}\right)+2T_{1b}\cos\alpha_{1b}\cos\gamma_{1b}\\ &\qquad -2V_{1b}\cos\phi_{1b}\cos\left(\delta_{1b}-\frac{2\pi}{n}\right)=0\\ &-2T_{1a}\sin\alpha_{1a}+2T_{1b}\sin\alpha_{1b}+2V_{1b}\sin\phi_{1b}=0\end{aligned}\right\} \quad (3)$$

Node 2_a:

$$\left.\begin{aligned} &-2T_{1b}\cos\alpha_{1b}\cos\left(\gamma_{1b}-\frac{2\pi}{n}\right)+2T_{2a}\cos\alpha_{2a}\cos\gamma_{2a}\\ &\qquad +V_{2a}\cos\phi_{2a}-B_1\cos\beta_1=0\\ &-2T_{1b}\sin\alpha_{1b}+2T_{2a}\sin\alpha_{2a}+V_{2a}\sin\phi_{2a}+B_1\sin\beta_1=0\end{aligned}\right\} \quad (4)$$

Node $2'$:

$$\left.\begin{aligned} &-V_{2a}\cos\phi_{2a}+2V_{2b}\cos\phi_{2b}\cos\delta_{2b}+2B_2\cos\beta_2\cos\delta_{2\beta2}-2H_2\sin\frac{2\pi}{n}=0\\ &V_{2a}\sin\phi_{2a}+2V_{2b}\sin\phi_{2b}+2B_2\sin\beta_2=0\end{aligned}\right\} \quad (5)$$

Node 2_b:

$$\left.\begin{aligned} &-2T_{2a}\cos\alpha_{2a}\cos\left(\gamma_{2a}-\frac{2\pi}{n}\right)+2T_{2b}\cos\alpha_{2b}\cos\gamma_{2b}\\ &\qquad -2V_{2b}\cos\phi_{2b}\cos\left(\delta_{2b}-\frac{2\pi}{n}\right)=0\\ &-2T_{2a}\sin\alpha_{2a}+2T_{2b}\sin\alpha_{2b}+2V_{2b}\sin\phi_{2b}=0\end{aligned}\right\} \quad (6)$$

Before solving the equations, it is necessary to determine the angle parameters. For example, if the span of the dome is 120 meters, and both the rise-span and thickness-span ratios are 0.07. Then, the vertical projection and horizontal projection of the components can be calculated. The angle parameters can be calculated based on the projection geometric relations. Finally, by incorporating the angle parameters into the nodal equilibrium equations, the relative internal force of the components can be obtained.

Assuming the internal force of the outer hoop cable H_2 is 10000 kN, the internal force of each component is obtained through nodal equilibrium equations. The results are shown in Table 2.

Table 2
Sectional size and initial pre-stress of the components

Component	Pre-stress (kN)	Cross-section (mm^2)
N_1	3711	Φ155
N_{1a}	4206	Φ155
T_{1a}	1196	Φ131
T_{1b}	1722	Φ131
T_{2a}	4108	Φ155
T_{2b}	3733	Φ155
V_{1a}	-156	Φ114 × 7.5
V_{1b}	-113	Φ114 × 7.5
V_{2a}	-1263	Φ630 × 11
V_{2b}	-449	Φ630 × 11
B_1	1086	Φ131
B_2	2823	Φ155
H_1	2085	Φ131
H_2	10000	Φ190

3. Load state analysis

3.1. Finite element model

The full-scale model used in this study is a stadium with a span of 120 meters and both rise-span and thickness-span ratios of 0.07. The cable dome model consists of 264 elements, 84 struts, 180 cables and 24 edge supports. The structure is divided into 12 substructures. The cables are made of steel strands, and the struts are made of Q345B seamless steel pipe. Material parameters can be found in Table 3. Boundary conditions are applied to Nodes 3a (Fig. 1c), restraining displacements in all directions (*X*, *Y* and *Z*) while allowing rotations (pin connection).

Furthermore, the structure underwent static analysis using ANSYS software, with the non-linear system of equations solved using the New-Raphson method. The struts and cables were simulated using Link180 and Link10 elements, respectively. Although research shows that tensioned membranes can improve the stiffness of a structure [26], the improvement observed in the study was insignificant. Therefore, the effect of tensioned membranes on the stiffness of the structure was not considered [27]. Moreover, the external load was applied to the nodes as the equivalent concentrated load.

Table 3
Material properties

Property	Cable	Strut
Steel grade	1860-grade steel	Q345B steel
Tensile strength (MPa)	1860	345
Poisson's ratio	0.3	0.3
Modulus of elasticity (MPa)	1.95×10^5	2.06×10^5
Coefficient of linear expansion	1.36×10^{-5}	1.2×10^{-5}
Density (kg/mm^3)	7.85×10^{-6}	7.85×10^{-6}

Load state analysis is carried out to investigate the static performance of the pentagonal three-four strut hybrid open-type cable dome. The initial live load is 0.6 kN/m², and the initial dead load is 0.1 kN/m². All load state analyses consider the effect of gravity.

The analysis includes four cases, which are defined as follows (where λ is the scale factor):

Case 1: DL 1 + λ × LL 1
Case 2: DL 1 + λ × LL 2
Case 3: 1.3 × DL 1 + 1.5 × LL 1
Case 4: 1.3 × DL 1 + 1.5 × LL 1 + 0.7 × 1.5 × WL 1
where DL 1: Full-span dead load
LL 1: Full-span live load
LL 2: Half-span live load
WL 1: Wind load (0.45 kN/m^2)

3.2. Full-span uniform load

In Case 1, as the vertical live load increases, the internal forces of the components and the displacement of nodes undergo changes (see Fig. 1b for node numbering, which applies for all cases) that are illustrated in Fig. 3.

1. Fig. 3a shows that as the vertical load increases, the internal forces of both the upper chord hoop cable and the ridge cable decrease. At a scale factor of λ=3.5, slackness occurs in the ridge cable, resulting in a decrease in the internal force of T_{1a} to 0. Additionally, the inner hoop experiences a higher rate of decrease compared to the outer hoop.
2. Fig. 3b and 3c demonstrate that as the vertical load increases, the internal forces of both the diagonal and hoop cables exhibit a lower rate of increase. Additionally, the inner hoop experiences a higher rate of increase compared to the outer hoop.
3. It can be seen from Fig. 3d that the internal forces of the struts increase, with the outer hoop exhibiting a higher rate of increase in comparison to the inner hoop.
4. Fig. 3e and 3f show that the maximum displacement occurs at nodes 1 and 2, and the maximum displacement increases with the increase of load. The maximum vertical displacement measures -285.708 mm, which is less than $L/250$ and complies with the limitation set by the standard "JGJ 257-2012 Technical Specification of Cable Structure". Notably, the changes in internal forces and displacements of the inner hoop components are significantly larger than those of the outer hoop.

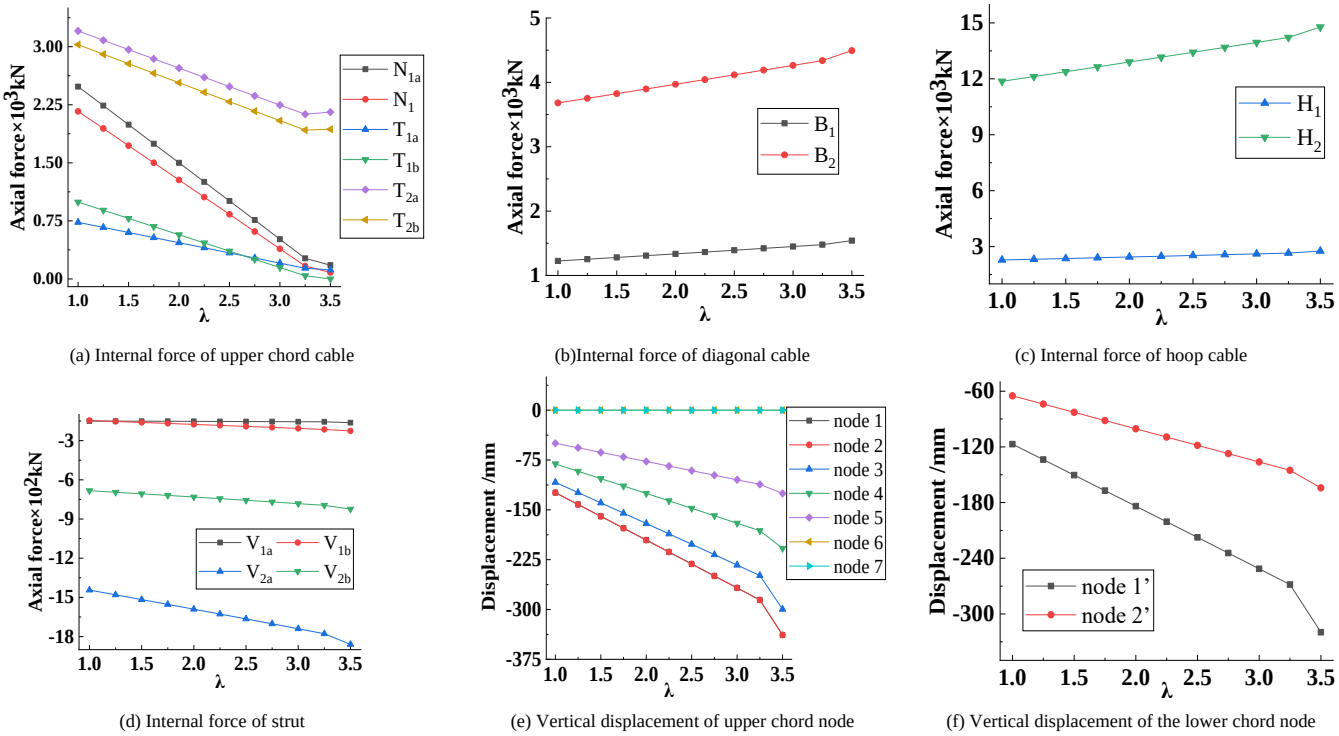

(a) Internal force of upper chord cable (b)Internal force of diagonal cable (c) Internal force of hoop cable

(d) Internal force of strut (e) Vertical displacement of upper chord node (f) Vertical displacement of the lower chord node

Fig. 3 Internal forces of components and nodal displacements under full-span uniform load

3.3. Half-span uniform live load

In Case 2, an asymmetric load analysis of the structure is carried out. The initial load comprises the dead load multiplied by 1.0 and the live load multiplied by 1.0. The live load is incrementally increased in steps (0.25 times per step). The changes in internal forces of components and nodal displacements are shown in Fig. 4 and 5. The results are summarized below.

1. As shown in Fig. 4a and 5a, the internal forces of the upper chord hoop cables and ridge cables show a decreasing trend with the increase of vertical load. Particularly, the internal forces of upper chord hoop cables N_1 and N_{1a} (span with live load) decrease significantly.
2. As shown in Fig. 4b, 4c, 5b and 5c, in the span without live load, the internal forces of both diagonal and hoop cables display a decreasing trend, while in the span with live load, the internal forces of diagonal and hoop cables display an increasing trend.
3. As shown in Fig. 4e, 4f, 5e and 5f, the nodal displacements in the span with live load show an increasing trend with the increase of live load, while the nodal displacements in the span without live load show a decreasing trend. At a scale factor of λ=1.75, an arching phenomenon appears in the span without live load. When the structure is subjected to 3.25 times the initial live load, the maximum vertical displacement of the structure occurs at the upper chord node 1, measuring 544.878 mm. This value exceeds the limit of L/250, indicating that it does not meet the requirements of the standard.

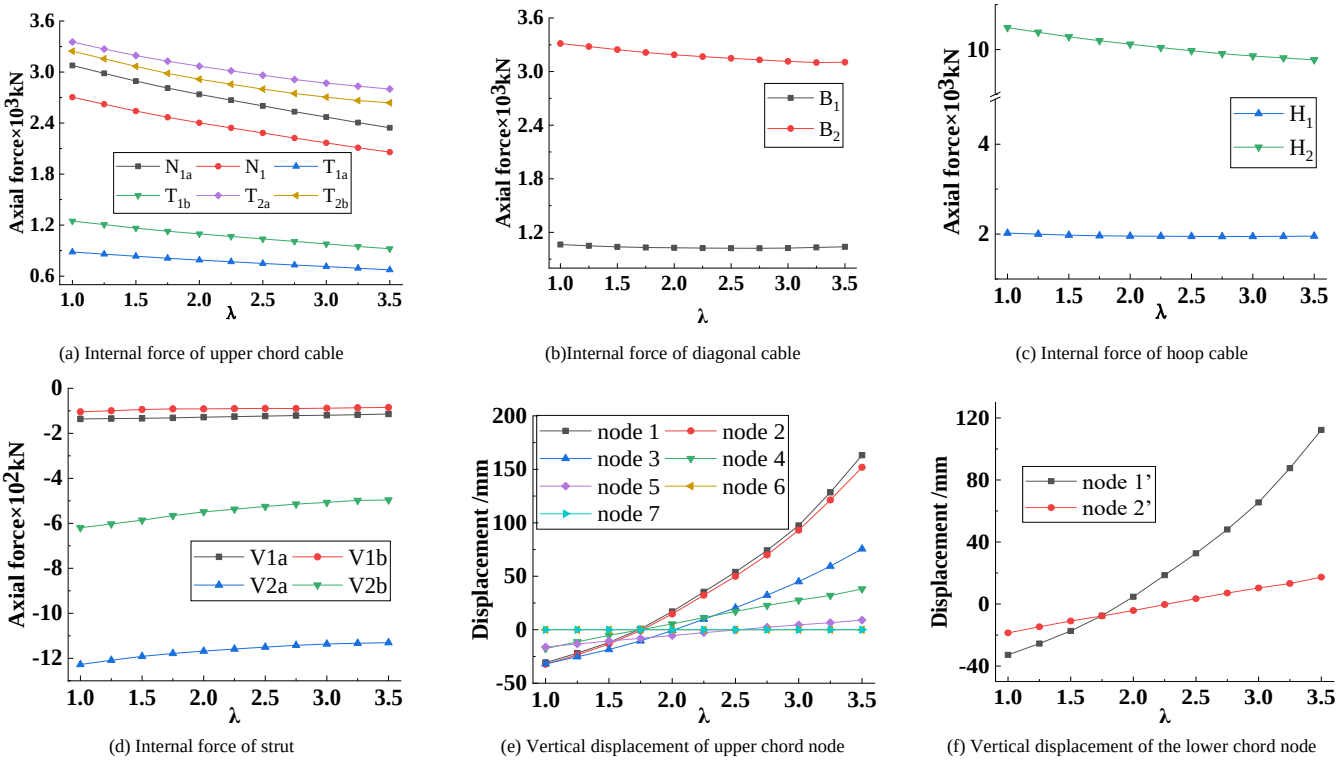

(a) Internal force of upper chord cable (b)Internal force of diagonal cable (c) Internal force of hoop cable

(d) Internal force of strut (e) Vertical displacement of upper chord node (f) Vertical displacement of the lower chord node

Fig. 4 Internal forces of components and nodal displacements under half-span load (span without live load)

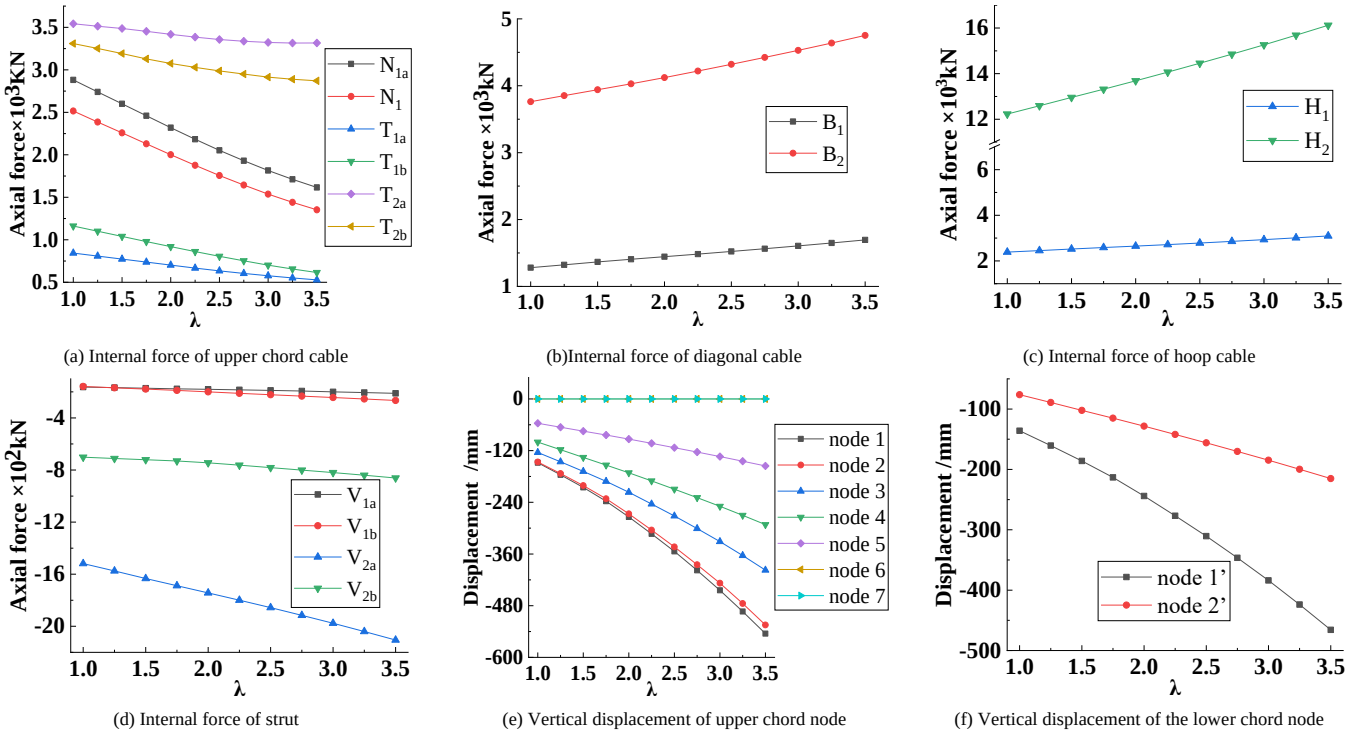

(a) Internal force of upper chord cable (b)Internal force of diagonal cable (c) Internal force of hoop cable

(d) Internal force of strut (e) Vertical displacement of upper chord node (f) Vertical displacement of the lower chord node

Fig. 5 Internal forces of components and nodal displacements under half-span load (span with live load)

A comparative analysis of Case 1 (Fig. 3) and Case 2 (Fig. 4) reveals that the deformation of the structure is uniform under full-span live load. However, when subjected to an asymmetric load, the deformation of the structure is undulating. In the case of half-span live load, the structure exhibits arching behavior. Under the full-span live load, the maximum vertical displacements appear at nodes 1 and 2. On the other hand, under the half-span live load, the maximum vertical displacement only occurs at node 1.

Ridge cable slackness was observed when the structure was subjected to 3.5 times the full span live load, indicating the significant influence of the pre-stress stiffness on the structure. Conversely, when the structure was subjected to 3.25 times the initial half-span live load, the deformation exceeded the limit of the standard, which indicates that the overall structural stiffness plays a dominant role at that point. The bearing capacity of the structure is reduced under asymmetric load conditions. Therefore, additional construction measures must be taken to mitigate the effect.

3.4. Wind load

In large spatial structures, roof wind pressure and wind suction have a significant impact on the structural cable tension strain [28]. Therefore, it is of practical significance for structural design to study the mechanical response of the pentagonal three-four strut hybrid open-type cable dome under wind load. The equivalent static wind load is calculated according to the " GB 50009-2012 Load code for the design of building structures", using the formula $\omega_k = \beta_Z \mu_S \mu_Z \omega_0$. The wind-induced vibration coefficient β_Z is determined as 1.0 based on wind tunnel test results and random vibration theory calculations for the flexible roof structure. The structural shape factor of wind load μ_S is set to -1.0, considering the overall flexibility of the cable dome. For a building height of 40 m and a ground roughness class of C, the wind pressure coefficient μ_Z is assigned a value of -1.0. The reference wind pressure ω_0 is determined to be 0.45 kN/m^2. The results of the comparative analysis between Case 3 and Case 4 are shown in Table 4.

Table 4
Internal forces of components under two cases

Parameters	Case 3 (kN)	Case 4 (kN)	Parameters	Case 3 (kN)	Case 4 (kN)
N_1	1216.49	2470.07	T_{2b}	2142.77	2743.43
N_{1a}	1423.74	2811.65	H_1	2215.40	1965.92
T_{1a}	440.70	805.54	H_2	11961.27	10640.71
T_{1b}	547.07	1119.30	V_{1a}	-137.30	-132.01
B_1	1208.13	1042.57	V_{1b}	-153.21	-110.93
B_2	3392.99	3030.60	V_{2a}	-1433.61	-1237.29
T_{2a}	2507.29	3120.05	V_{2b}	-509.82	-463.74

Note: N_1, N_{1a}-Upper chord hoop cable; T_{ia}, T_{ib}-Ridge cable; B_i-Diagonal cable; H_i-Hoop cable; V_{ia}, V_{ib}-Strut.

The internal forces in the upper chord hoop cable and ridge cables nearly doubled under wind loads. Furthermore, when the structure is subjected to wind load, the maximum vertical displacement is -38.93 mm, whereas in the absence of wind load, the maximum vertical displacement is -134.58 mm. This substantial reduction in the maximum vertical displacement of the structure highlights the favorable impact of wind load on its structural behavior. The displacement is reduced by nearly 70%, which indicates that the structure is highly sensitive to wind load.

3.5. Effect of temperature on the static performance of the structure

The effect of temperature loads on pre-stress large spatial structures should not be disregarded. In certain super-stationary structural systems, temperature stresses surpass the load stresses. Consequently, temperature loads have become the governing condition for determining the structural bearing capacity when considering load combinations. The fundamental impact of temperature on pre-stress structural systems is attributed to the thermal expansion and contraction of materials, causing the material to develop an inelastic shape. However, due to the presence of boundary constraints and mutual restraint between individual components, the free expansion or contraction are restricted, resulting in the generation of temperature stresses that ultimately affect the structural performance [29].

The annual mean temperature in China is 9.55°C, with a maximum temperature of 49.6°C and a minimum temperature of -52.3°C [30, 31]. The temperature of the component is closely influenced by the ambient temperature. In general, the surface temperature of steel tends to be 2-3°C higher than the surrounding air temperature [32]. If exposed to direct sunlight, the surface temperature of components can rise by 8-12°C compared to the ambient temperature. This study analyzes the effects of temperature on the structural performance within a temperature range of -60°C to 60°C. The structure under investigation is subjected to a uniformly distributed load of 0.7 kN due to gravity. Additionally, a pre-stress of 10,000 kN is applied to the outer hoop cable H_2. Fig. 6 shows the change in internal forces of the components and nodal displacements under different temperature loads. The conclusions are as follows:

1. With an increase in temperature, the internal forces of the struts consistently exhibit a decreasing trend (Fig. 6a-d). Notably, the outer hoop components are more sensitive to temperature variations compared to the inner loop components. The changes in internal forces in the components are significantly larger in the outer hoop than in the inner hoop.
2. When the temperature reaches 50°C, the ridge cable T_{1a} slacks, leading to a sudden change in the nodal displacement (Fig. 6a). To eliminate the

adverse effect of high temperature on the structural bearing capacity, it is recommended to appropriately increase the pre-stress level.

3. When the temperature increases, the internal force of the components decreases, and the vertical displacement decreases correspondingly (Fig. 6a-f). The reason is attributed to the diminishing contribution of pre-stress stiffness and the gradual dominance of structural stiffness.

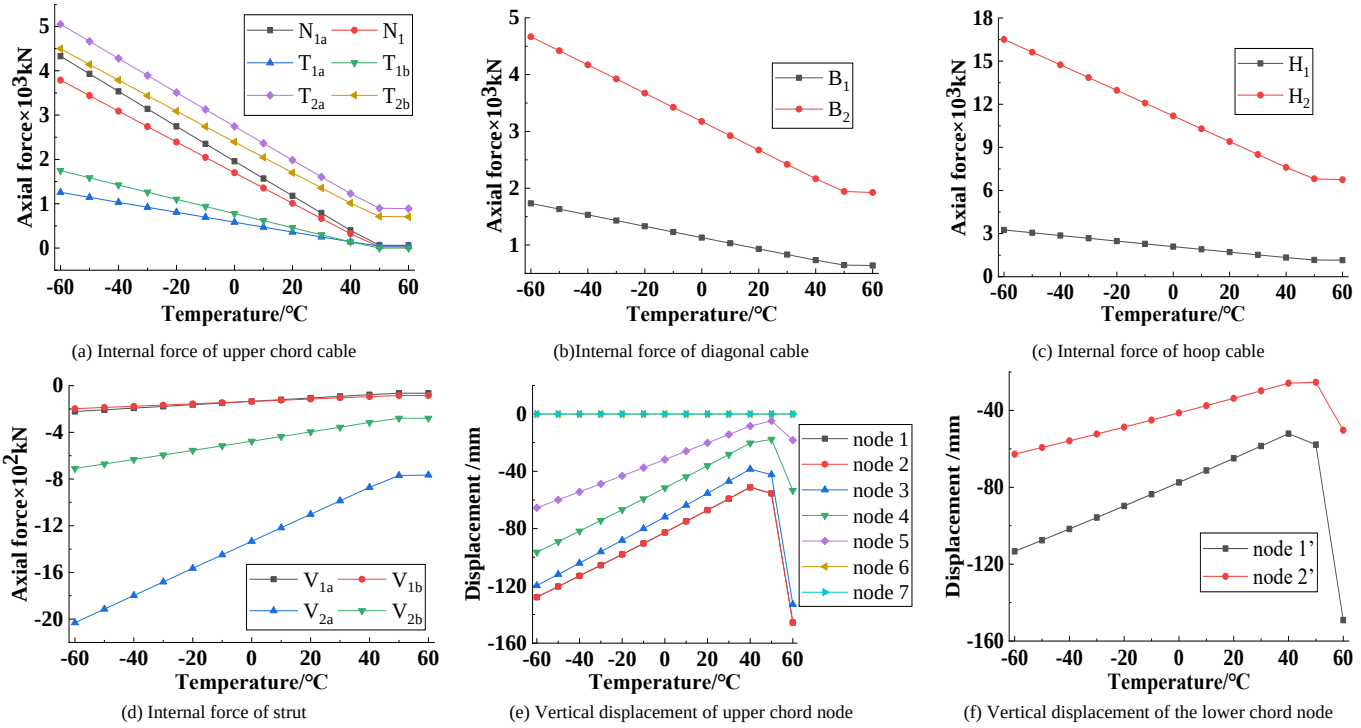

(a) Internal force of upper chord cable (b)Internal force of diagonal cable (c) Internal force of hoop cable

(d) Internal force of strut (e) Vertical displacement of upper chord node (f) Vertical displacement of the lower chord node

Fig. 6 Internal forces of components and nodal displacement response at different temperatures

4. Parametric analysis

The performance of the cable dome structure is closely linked to its topological configuration, pre-stress distribution and pre-stress level. Therefore, it is indispensable to examine the influence of these parameters on the overall performance of the cable dome. To further explore the static characteristics of the novel cable dome, this study specifically focuses on analyzing the effects of three key parameters: rise-span ratio, thickness-span ratio and pre-stress level on the structural performance under the load conditions of case 1.

4.1. Rise-span ratio

The effect of the structural rise-span ratio ($f/L = 0.06,\ 0.07,\ 0.08,\ 0.09,\ 0.10$) on structural performance is discussed. The changes in internal forces of the components are shown in Fig. 7a-d and the response of nodal displacements in Fig. 7e-f. The following conclusions can be drawn:

1. As the rise-span ratio increases, the internal forces of all components decrease. The highest rate of change in internal force is observed in the upper chord hoop cable N_{1a}. Furthermore, the structural pre-stress distribution becomes more uniform.
2. The larger the rise-span ratio, the smaller the structural deformation.
3. With an increase in the rise-span ratio, the vertical nodal displacement becomes smaller, suggesting that appropriately increasing the rise-span ratio is beneficial to minimizing structural deformation.

However, as the rise-span ratio increases, the pre-stress of the upper chord cable decreases, resulting in a reduction in the stiffness of the structure. To prevent cable slackening, it is recommended to maintain the rise-span ratio within the range of 0.07 to 0.08.

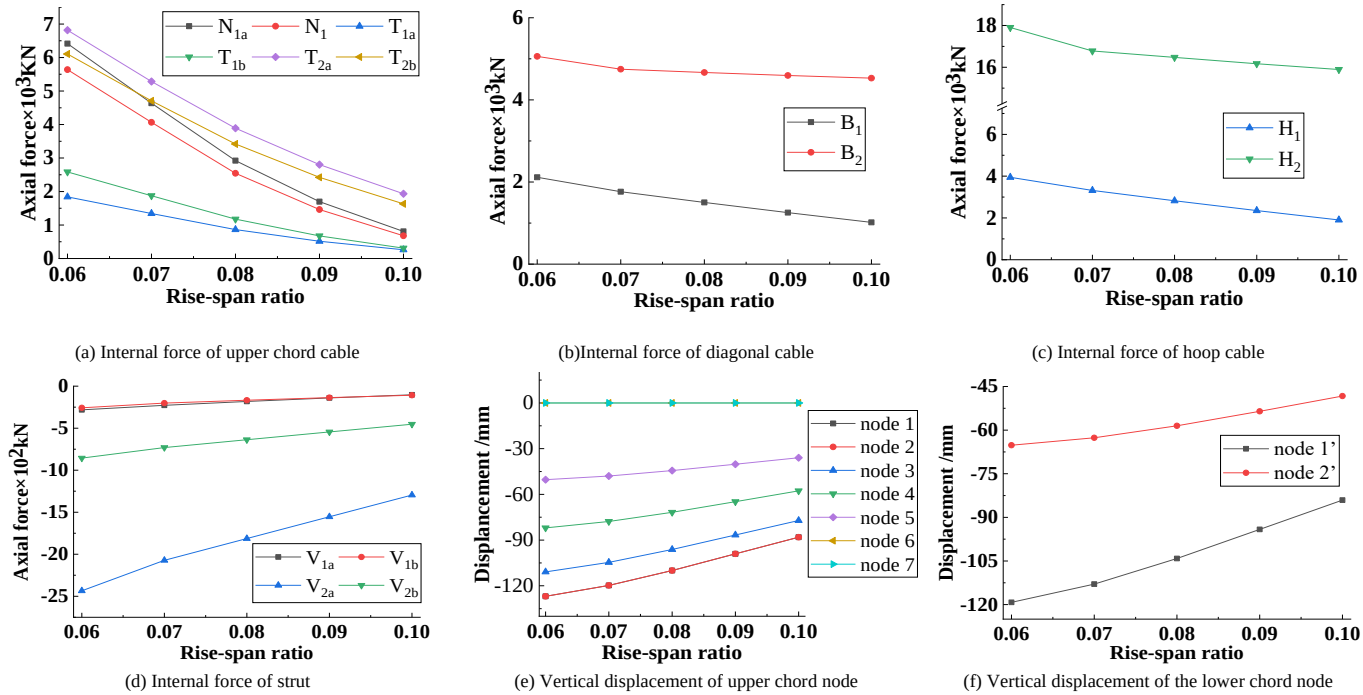

(a) Internal force of upper chord cable (b)Internal force of diagonal cable (c) Internal force of hoop cable

(d) Internal force of strut (e) Vertical displacement of upper chord node (f) Vertical displacement of the lower chord node

Fig. 7 Internal forces of components and nodal displacement response with the different rise-span ratios

4.2. Thickness-span ratio

The response of internal forces of the components and the vertical nodal displacements as the thickness-span ratio increases is shown in Fig. 8. With an increase in thickness-span ratio, the internal forces of the upper chord cables increase. Specifically, the internal forces of N_1 and N_{1a} are increased by 1600 kN and 1500 kN, respectively. Furthermore, it is observed that when the thickness-span ratio reaches 0.09, the internal force of N_1 exceeds that of T_{2a}.

As the thickness-span ratio increases, the internal forces of the components generally increase. However, it is important to note that the internal force of the components does not increase uniformly with the increase in the thickness-span ratio. Specifically, in the case of the outer hoop cable H_2, its internal force exhibits an increasing trend initially and then a decreasing trend (Fig. 8b). Increasing the thickness-span ratio can effectively reduce the vertical nodal displacement. As the thickness-span ratio increases, the vertical displacements of the upper and lower chord nodes decrease. Additionally, it is observed that the vertical displacements of the inner hoop nodes are significantly greater than those of the outer hoop nodes, indicating that the inner hoop components are more sensitive to changes in the thickness-span ratio (Fig. 8d, 8f). As the thickness-span ratio increases, the nodal displacements of the structure decrease and the internal forces of the ridge cables increase. This indicates that moderately increasing the thickness-span ratio can enhance the structural stiffness. Considering the structural cost and construction convenience, it is recommended to have a thickness-span ratio within the range of 0.06-0.08. At this range, the pre-stress forces are evenly distributed throughout the structure.

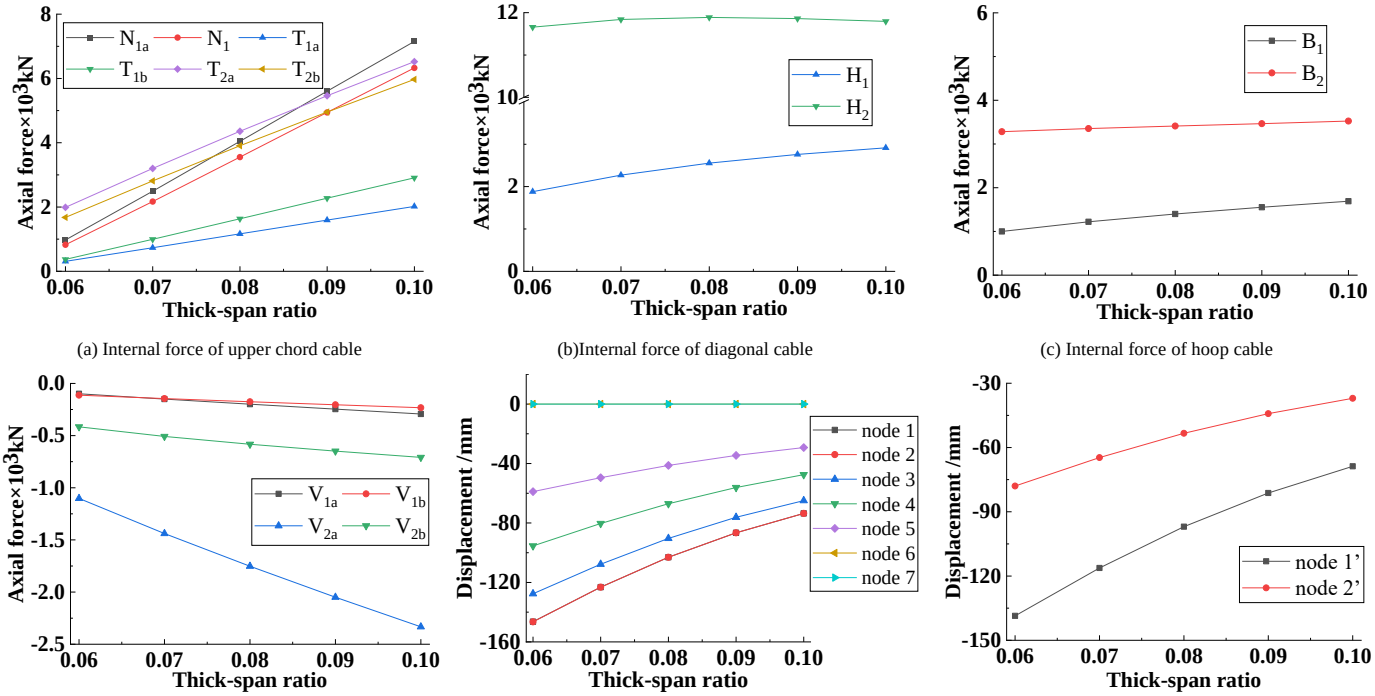

(a) Internal force of upper chord cable (b)Internal force of diagonal cable (c) Internal force of hoop cable

(d) Internal force of strut (e) Vertical displacement of upper chord node (f) Vertical displacement of the lower chord node

Fig. 8 Internal forces of components and nodal displacement response with the different thick-span ratios

4.3. Pre-stress Level

The change in internal forces of the structure and nodal displacements under different pre-stress levels is shown in Fig. 9.

1. It can be seen from Fig. 9a-d that as the initial pre-stress increases, the internal forces of all components continuously increase. The rate of change in the inner hoop ridge cables and struts is slower than that of the outer hoop ridge cables and struts.
2. From Fig. 9e-f, it is evident that the nodal displacement decreases as the initial pre-stress increases, and the decreasing trend becomes gentler with each increment.

The vertical displacement of the structure decreases as the structural pre-stress level increases. This indicates that increasing the pre-stress level can improve the structural stiffness and prevent slackness in the ridge cables. However, it is vital to ensure that the pre-stress level does not exceed the breaking force of the cables. Additionally, increasing the pre-stress level will lead to higher construction costs.

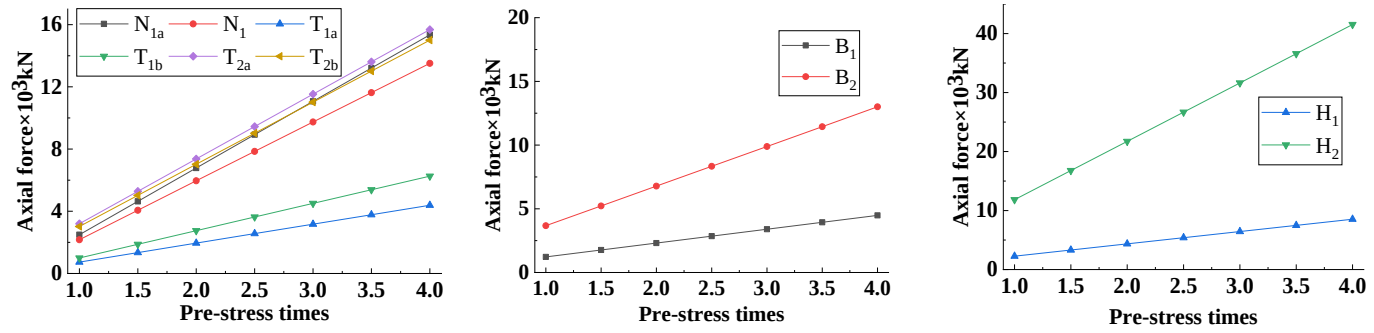

(a) Internal force of upper chord cable (b) Internal force of diagonal cable (c) Internal force of hoop cable

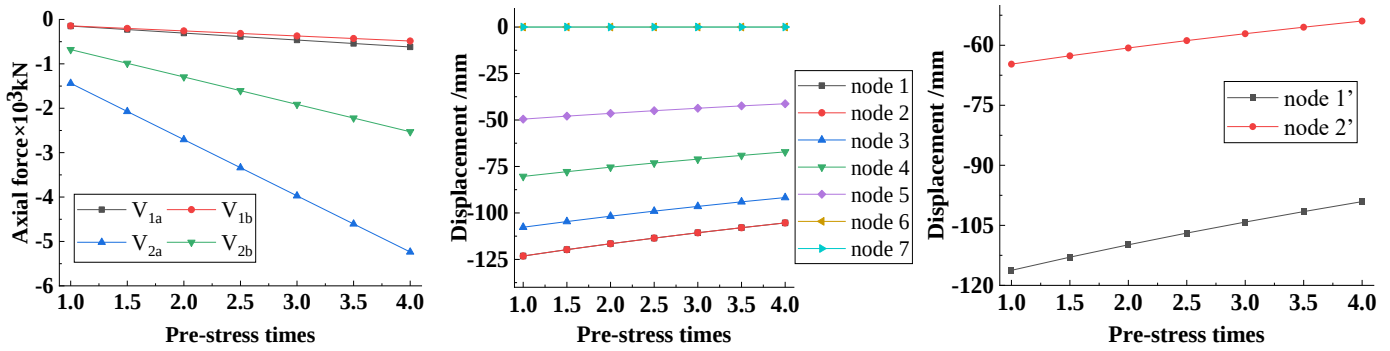

(d) Internal force of strut (e) Vertical displacement of upper chord node (f) Vertical displacement of the lower chord node

Fig. 9 Internal forces of components and nodal displacement response with different pre-stress multipliers

5. Conclusions

This study proposes a new cable dome design known as the pentagonal three-four strut hybrid open-type cable dome. The primary focus of the research is on conducting a topology analysis of this innovative cable dome structure. Based on the nodal equilibrium equations, the pre-stress state of the structure is determined. Furthermore, load state analysis and parametric analysis are conducted to evaluate the structural performance of the cable dome. The main conclusions of this paper are as follows:

Compared to the traditional cable dome, the structural performance of the new one is more advanced. Its strut-cable ratio is greater than that of the Levy-type cable dome and the Geiger-type cable dome. Under the same mass condition, the cost of the cable is 2.5 times higher than that of the steel pipe. Therefore, the new structure is more cost-effective.

The high-temperature load weakens the stiffness of the structure, while the low-temperature load strengthens it. The initial pre-stress design of the cable dome should consider the effect of temperature load on stiffness. To mitigate the impact of extreme weather, it is necessary to strengthen the pre-stress stiffness of the structure.

When subjected to significant asymmetric loads, the maximum nodal displacement exceeds the limit of the standard. Therefore, structural deformation should be monitored during the installation of the membrane. Engineers and workers can divide the cable dome into designated areas and install membranes simultaneously in symmetrical areas.

The structure is sensitive to wind load. Appearance design should be considered to reduce the adverse effect of wind loads.

Appropriate adjustment of the rise-span ratio, thickness-span ratio and pre-stress level can optimize the structural performance. Considering factors such as construction cost and convenience, this paper recommends a pre-stress level ranging from 1.2 to 1.5 times, a rise-span ratio ranging from 0.07 to 0.08 and a thickness-span ratio ranging from 0.06 to 0.08.

Acknowledgments

The work was financially supported by the National Natural Science Foundation of China (No. 52268031), the Jiangxi Province University Humanities and Social Sciences Research Project (No. YS22113) and the Intelligent Building Engineering Research Center of Jiangxi Province Open Fund (No. HK20213005), which is gratefully acknowledged.

References

[1] Hui. Deng, M.R. Zhang, H.C. Liu, et al., "Numerical Analysis of the Pretension Deviations of a Novel Crescent-shaped Tensile Canopy Structural System", Engineering Structures, 119, 24-33, 2016.
[2] T.N. Zhang, J.Y. Zhao, "Seismic Resilience Assessment of a Single-layer Reticulated Dome During Construction", Advanced Steel Construction, 19(1), 77-85, 2023.
[3] X.Y. Fu, Y. Gao, C.Z. Xiao, et al., "Horizontal Skyscraper: Innovative Structural Design of Shenzhen VANKE Center", Journal of Structural Engineering, 138(6), 663-668, 2012.
[4] S.J. Sun, K.H. Mei, Y.M. Sun, et al., "Structural Performance of Super-Long-Span Cable-Stayed Bridges with Steel and CFRP Hybrid Cables", Arabian Journal for Science and Engineering, 45(5), 3569-3579, 2019.
[5] M.M. Ding, Bin. Luo, S.Y. Ding, et al., "Experimental Investigation and Numerical Simulation of a Levy Hinged-Beam Cable Dome", Buildings, 11(3), 2021.
[6] H.H. Ma, Y.Y. Ma, Feng. Fan, et al., "Seismic performance of single-layer spherical reticulated shells considering joint stiffness and bearing capacity", Advanced Steel Construction, 18(2), 604-616, 2022.
[7] Jian. Lu, S.D. Xue, X.Y. Li, et al., "Segmented Assembly Construction Forming Method Without Brackets of Spatial Cable-Truss Structure Without Inner Ring Cables", Advanced Steel Construction, 18(3), 687-698, 2022.
[8] L.M. Tian, J.P. Wei, Q.X. Huang, et al., "Collapse-Resistant Performance of Long-Span Single-Layer Spatial Grid Structures Subjected to Equivalent Sudden Joint Loads", Journal of Structural Engineering, 147(1), 2021.
[9] Jie. Wu, "Cable Force Characteristic Test of Bidirectional Beam String Structure after Cable Shape Optimization", Journal of Tianjin University(Science and Technology), 49(1), 86-95, 2016.
[10] Z.L. Zong, Z.X. Guo, F.W. Lv, "Experimental Research on A Composite Structure of Cable Dome and Rigid Shell", Journal of Zhejiang University (Engineering Science), 29(7), 75-79, 2013.
[11] Feng. Fan, Li. Cai, "Static Analysis of Inclined-strut System Cable Dome", Journal of Harbin Institute of Technology, 40(6), 841-845, 2008.
[12] Yu. Fang, C.W. Huang, T.W. Zhou, et al., "Parameter Analysis of Rigid Kiwitt Dome Structure", Industrial Construction, 46, 313-316, 2016.
[13] Hui. Wu, D.Q. Cen, B.Q. Gao, "Approximate Optimization and Performance Analysis of Rigid Cable Dome Structure", Journal of Zhejiang University (Engineering Science), 45(11), 1966-1971, 2011.
[14] A.L. Zhang, C.Q. Wu, Y.X. Zhang, "Analysis on the Structure and Initial Prestress of T-Type Three Strut Cable Dome", Journal of Beijing University of Civil Engineering and Architecture, 37(1), 01-07, 2021.
[15] S.L. Dong, W.G. Chen, Yuan. Tu, et al., "Configuration and Prestressing Distribution of the Honeycomb-type Cable Dome with Three Struts", Engineering Mechanics, 36(9), 128-135, 2019.
[16] S.L. Dong, Y.D. Wang, H.C. Liu, "Structural Form Innoivation and Initial Prestress Analysis on Drum-shaped Honeycomb-type Cable Domes with Multi-strut Layout ", Spatial Structures, 28(3), 3-15, 2022.
[17] A.L. Zhang, W.J. Yuan, Y.X. Zhang, et al., "Static Performance Analysis of Alternated Cable Dome with Single and Double Brace Struts", Journal of Vibration and Shock, 41(12), 321-330, 2022.
[18] H.Z. Bao, S.L. Dong, "Analyses on Functions of Static Mechanic in Bird-nest Cable Dome", Building Structure, 38(11), 11-13+39, 2008.
[19] S.L. Dong, W.G. Chen, Yuan. Tu, et al., "Analysis of Multi-parameter Sensitivity and Prestressing Force Distribution of Sunflower-type Cable Dome with Double struts", Journal of Tongji University(Natural Science), 47(6), 739-746+801, 2019.
[20] A.L. Zhang, L.N. Zhu, Y.X. Zhang, et al., "Configuration and Prestress Analysis Method of Star Shaped Tetrahedral Cable Dome", Journal of Vibration and Shock, 40(9), 84-91, 2021.
[21] S. Kmet, M. Mojdis, "Adaptive Cable Dome", Journal of Structural Engineering, 141(9), 2015.
[22] M.S. Chen, Ling. Yue, "Static Performance Analysis of Geiger-type Cable Dome", Journal of Hunan Institute of Engineering(Natural Science Edition), 25(4), 73-77, 2015.
[23] Shu. Yao, Fan. Feng, "Static Analysis of K6 Suspen·Dome Structure", Building Structure, 38(2), 43-46, 2008.
[24] R.W. Tang, X.Z. Zhao, Z.Y. Shen, "Factor Analysis of Geiger Cable Dome", Building Science, 29(1), 11-14+10, 2013.
[25] Yue. Feng, X.F. Yuan, A. Samy, "Analysis of New Wave-curved Tensegrity Dome", Engineering Structures, 250, 113408, 2022.
[26] W.T. Yan, H.B. Zhang, "Analysis of Form-finding of Cable Dome Supporting Membrane Structures", Steel Construction, 23(4), 1-3, 2008.
[27] L.L. Zhang, Chong. Ma, Yuan. Cao, et al., "Structural Stiffness of Tensioned Membrane Structure and Its Effect on the Structure Properties", Building Structure, 47(21), 25-29, 2017.
[28] Yue. Yin, W.J. Chen, J.H. Hu, et al., "In-situ Measurement of Structural Performance of Large-span Air-supported Dome under Wind Loads", Thin-Walled Structures, 169, 108476, 2021.
[29] Zhong. Fan, Zhe. Wang, Jie. Tang, "Analysis on Temperature Field and Determination of Temperature upon Healing of Large-span Steel Structure of the National Stadium", Journal of Building Structures, 28(2), 32-40, 2007.
[30] C.H. Ye, J.Z. Lv, Z.G. Lin, "A Study on New Extreme Maximum Air Temperature in China", Meteorological Monthly, 34(11), 3-6, 2008.
[31] Y.J. Zhao, Cheng. Chang, C.Y. Bai, et al., "Climate Characteristic and Change of Mohe Extreme Temperature", Meteorological Monthly, 35(3), 94-98, 2009.
[32] A.L. Zhang, X.C. Liu, Shan. Feng, et al., "Temperature Response Analysis of Large-Span Cable Dome Structure", Journal of Building Structures, 33(4), 40-45, 2012.